

UC Riverside

UC Riverside Previously Published Works

Title

Leveraging Electron Transfer Dissociation for Site Selective Radical Generation: Applications for Peptide Epimer Analysis

Permalink

<https://escholarship.org/uc/item/2rx8z99k>

Journal

Journal of The American Society for Mass Spectrometry, 28(7)

ISSN

1044-0305

Authors

Lyon, Yana A
Beran, Gregory
Julian, Ryan R

Publication Date

2017-07-01

DOI

10.1007/s13361-017-1627-x

Peer reviewed



Published in final edited form as:

J Am Soc Mass Spectrom. 2017 July ; 28(7): 1365–1373. doi:10.1007/s13361-017-1627-x.

Leveraging Electron Transfer Dissociation for Site Selective Radical Generation: Applications for Peptide Epimer Analysis

Yana A. Lyon¹, Gregory Beran¹, and Ryan R. Julian^{1,*}

¹Department of Chemistry, University of California, Riverside, 501 Big Springs Road, Riverside, CA 92521, USA

Abstract

Traditional electron-transfer dissociation (ETD) experiments operate through a complex combination of hydrogen abundant and hydrogen deficient fragmentation pathways, yielding c and z ions, side chains losses, and disulfide bond scission. Herein, a novel dissociation pathway is reported, yielding homolytic cleavage of carbon-iodine bonds via electronic excitation. This observation is very similar to photodissociation experiments where homolytic cleavage of carbon-iodine bonds has been utilized previously, but ETD-activation can be performed without addition of a laser to the mass spectrometer. Both loss of iodine and loss of hydrogen iodide are observed, with the abundance of the latter product being greatly enhanced for some peptides after additional collisional activation. These observations suggest a novel ETD fragmentation pathway involving temporary storage of the electron in a charge-reduced arginine side chain. Subsequent collisional activation of the peptide radical produced by loss of HI yields spectra dominated by radical-directed dissociation, which can be usefully employed for identification of peptide isomers, including epimers.

Introduction

Radical chemistry has played an important role in the development of mass spectrometry over the years, and the combination continues to evolve and produce useful applications. Unfortunately, many modern ionization sources are geared towards gentle transfer of large biomolecular ions into the gas phase, and do not typically generate odd-electron ions in significant abundance.¹² Methods for introducing radicals post-ionization are therefore required. Several options are available, including photodissociation³ and collisional-activation based approaches.^{4–6} Radical chemistry can also be combined with ion-ion reactions utilizing either activation method.⁷ Once created, odd-electron chemistry has many uses in the gas phase including: cross-linking,⁸ examining three dimensional structure,⁹ accessing novel dissociation pathways,^{10,11} and isomer identification.¹² Radical-directed dissociation (RDD) is often sensitive to fine structural details because dissociation is preceded by radical migration, which is guided by the relative orientation of hydrogen atom(s) that must be abstracted to allow relocation of the nascent radical to the ultimate site of fragmentation.¹³

*corresponding author: ryan.julian@ucr.edu.

A key for many of these applications is site-specific generation of a radical via homolytic photodissociation of labile bonds. Dissociation occurs due to electronic excitation to dissociative excited states, leading to fragmentation on the femtosecond timeframe.¹⁴ Many bonds have been demonstrated to be suitable, including carbon-iodine, carbon-sulfur, and sulfur-sulfur.¹⁵ In optimal cases, radical yields can be quantitative with a single laser pulse,¹⁶ but implementation requires coupling an ultraviolet laser to a mass spectrometer—an experimental configuration that is not currently commercially available. The need for customized instrumentation has likely limited accessibility to the technique.

In contrast, electron-transfer dissociation (ETD) is another radical based fragmentation method that is widely available on many commercial platforms. ETD was developed following discovery of electron capture dissociation (ECD),¹⁷ and both facilitate fragmentation by delivering an electron to a multiply charged cation, often yielding very similar results. In ETD, the electron originates from a molecular anion and transfer results in charge reduction, energy increase, and dissociation. For peptides, fragmentation into *c/z* ions typically dominates, with the side benefit that post-translational modifications (PTMs) are often preserved.¹⁸ ETD can also be used to identify isomers, such as iso-aspartic acid, for which a unique fragment ion is generated.¹⁹ ECD has been used to interrogate three-dimensional protein structure by mapping out the relative strength of noncovalent interactions between sequence remote regions.²⁰ Thus, there are many similarities between applications of RDD and ETD/ECD. Interestingly, electron transfer also converts an ion into a hydrogen abundant radical, which can spontaneously convert into a hydrogen deficient radical, the same type of radical operative in RDD. Indeed, some of the fragmentation observed in ETD/ECD is attributable to RDD,²¹ but precise mechanisms accounting for all observed fragmentation in ETD/ECD are not universally agreed upon and have been the source of significant study and controversy.²²

In the present work, we present a method for generating site-specific cleavage of carbon-iodine bonds via ETD rather than photodissociation. Both homolytic cleavage due to excitation of dissociative electronic states yielding loss of iodine radical ($-I^{\bullet}$), and loss of iodine accompanied by hydrogen ($-HI$) are observed. Interestingly, the ratio of these two losses varies as a function of additional collisional activation, with the amount of $-HI$ loss increasing dramatically with greater activation for some peptides. A novel electron storage mechanism involving the side chain of arginine, which allows decoupling in time of electron transfer and dissociation, is proposed to account for these observations. Density-functional calculations support the proposed mechanism. Finally, the utility of ETD-generated radicals for isomer identification is illustrated by examination of several peptide isomers, dissimilar in structure due to isomerization or epimerization at a single residue. For these applications, the ability to simultaneously generate both even- and odd-electron species is shown to be beneficial in some cases.

Experimental

Materials

Organic solvents were purchased from Sigma Aldrich (St. Louis, MO) or Fisher Scientific and used without further purification. Water was purified to 18.2 M Ω by a Millipore 147

(Billerica, MA) Direct Q system. Amino acids and resins were purchased from Anaspec (Fremont, CA). Trypsin and urea were purchased from Sigma Aldrich (St. Louis, MO).

Peptide and Radical Precursor Synthesis

All synthetic peptides were synthesized manually using standard Fmoc procedures with Wang and Rink-Amide Resins as the solid support.²³ N-hydroxysuccinimide (NHS) activated iodobenzoyl esters were synthesized by following a previous procedure.¹⁶ Chloramine-T, sodium metabisulfite, and sodium iodide were purchased from Fisher Chemical (Fairlawn, NJ). Water was purified to 18.2 M Ω resistivity using a Millipore Direct-Q (Millipore, Billerica, MA). Peptides were iodinated by modification of a previously published procedure.³

Mass Spectrometry and dissociation of the peptides

Mass spectrometric analysis was performed using an Orbitrap Fusion Tribrid mass spectrometer (Thermo Fisher Scientific, San Jose, CA). Solutions containing ~1 μ M of protein in 49.5:49.5:1 MeCN/H₂O/AcOH were directly infused using the Nanospray Flex Ion source (Thermo Scientific, San Jose, CA) at 2 μ L per min through a 500 μ L syringe. 10 μ m ID emitters were pulled using a laser-based micropipette puller (Sutter Instrument, Novato, CA). Higher energy collision induced dissociation (HCD) was used for the supplemental activation (from 0 to 35 normalized collisional activation) in ETD which is termed EThcD. For ETD and EThcD experiments, 100 ms was used for fluoranthene reagent and peptide ion reaction time. The isolation window used for each step was 2–3 m/z to maximize ion count. For ETD-CID experiments, ETD or EThcD was first performed to generate the -I/-HI losses, then these peaks were isolated and subjected to collision induced dissociation (CID) of appropriate energy.

R_{isomer} calculations

To quantify isomer identification, an R_{chiral} value approach, originally reported by Tao *et al.*, was utilized.²⁴ In this paper, R_{isomer} represents the ratios of the relative intensities of a pair of fragments that varies the most between two isomers (R_A/R_B). If R_{isomer} = 1 then there the two mass spectra are the same and the species are not distinguishable. If R_{isomer} > 1, a larger number indicates a better degree of recognition. CID and RDD values were calculated using the +1 precursor charge state, while ETD-CID was performed on the +2 as charge reduction to the +1 occurs before dissociation.

Calculations

Theoretical calculations were carried out using density functional theory as implemented in Gaussian09.²⁵ The B3PW91 functional was used with the following basis sets: LANL2DZ²⁶ for iodine loss, 6-31+G(d) for disulfide cleavage, 6-31G(d) for c/z dissociation. Transition states were found using the QST3 approach and verified by calculating vibrational frequencies, for which a single imaginary value was obtained. The transition state for electron transfer to the disulfide functionality was not well behaved, and was therefore approximated via a step-wise scan of S-S bond length with all other coordinates relaxed.

Time-dependent density functional theory at the B3LYP/LANL2DZ level was used to optimize the lowest-energy excited state of iodobenzene.

Results and Discussion

ETD on the 2+ charge state of 4-iodobenzyl-modified VQEDFVEIHGK yields the spectrum shown in Figure 1a. As expected for an ETD experiment, c and z ions and an abundant charge reduced peak, corresponding to ETnoD,²⁷ are generated. However, the most abundant fragment results from loss of iodine, which is not a dissociation pathway previously observed to be abundant in ETD/ECD experiments. Closer examination, as shown in the inset of Figure 1a, reveals that the loss of both iodine and HI are observed. The high intensity of these losses implies that they are produced via energetically favorable pathways. An obvious possibility would be transfer of an electron (i.e. during the ET part of ETD) to the iodo-functional group, facilitating loss of iodine. Indeed, addition of an electron to iodobenzene in *ab initio* calculations leads to spontaneous loss of iodide anion upon minimization as shown in Figure 1b. This prediction by theory is also in agreement with previous experiments.²⁸ The product following electron attachment is iodide anion, which is unlikely to be lost from a doubly protonated peptide due to strong Coulombic attraction. However, intramolecular transfer of a proton to the iodide anion would yield HI, which should be less strongly bound and is an observed dissociation channel. This pathway for the generation of HI loss is illustrated in the upper path of Scheme 1.

The loss of neutral iodine is also observed in Figure 1a and is more difficult to explain because, as mentioned above, direct interaction of the electron with the iodobenzyl moiety should lead to dissociation of negatively charged iodide, not neutral iodine. Furthermore, iodide anion would not be expected to relinquish an electron back to the peptide. TDDFT calculations on iodobenzene reveal the first excited electronic state has HOMO→LUMO transition character. Relaxation on this excited state via geometry optimization yields dissociation along the C-I bond and prompt loss of neutral iodine, see Figure 1c. This same pathway is frequently accessed in photodissociation experiments, where the dissociative state is populated via absorption of a UV photon.¹⁶ In order to account for the neutral iodine loss in ETD, we propose that electron transfer leads to temporary occupation of an excited state by the excess electron, which subsequently decays to a lower energy state while simultaneously exciting an electron in the iodobenzyl group, prompting homolytic cleavage of the C-I bond. This type of energy coupling between separate excited state electrons has been observed previously in the context of energy transfer.²⁹

Another potential route for HI loss is illustrated in the lower portion of Scheme 1. If the transferred electron is captured at the protonated side chain of lysine or the N-terminus, a hypervalent amine is generated, which could subsequently attack the iodobenzyl moiety, leading to loss of HI. This mechanism would likely require close proximity between the protonated and iodobenzyl groups. In order to explore the feasibility of the two pathways shown in Scheme 1, experiments utilizing supplemental activation were carried out on 4IB-YLRPPSFLR-NH₂ and the results are shown in Figure 2. Less fragmentation is observed for this peptide compared to 4IB-VQEDFVEIHGK, but loss of iodine is still one of the most abundant pathways. ETD without additional activation is shown in Figure 2a. On the right

side of Figure 2 the ratio of I/HI loss is illustrated in the zoomed in spectra. With no additional activation, the loss of HI is minimal for 4IB-YLRPPSFLR-NH₂. However, with increasing collisional activation energy, the relative amount of HI loss increases dramatically. At the highest activation energy, loss of HI/I becomes the most abundant fragmentation channel (Figure 2e). There are two likely explanations that could account for these observations. First, it is possible that HI is created immediately after electron transfer, but not observed due to retention by noncovalent bonds.³⁰ Second, it is possible that HI is not generated until additional activation is applied.

Examination of the ratios of HI loss to c₇⁺ or c₈⁺ in the 4IB-YLRPPSFLR-NH₂ peptide reveals that the relative abundance of HI increases dramatically with increasing activation energy while the relative abundance of c-type ions remains relatively flat (see SI Figure 1), which supports delayed generation of HI. Collision-induced dissociation of the -HI/I products reveals a dissociation spectrum that is similar to what is seen when performing radical-directed dissociation (RDD), where the radical was generated by photodissociation (see Figure 3). In other words, ETD can be used for cleavage of the C-I bond, eliminating the need for a laser to carry out RDD experiments. Applications for this new fragmentation technique are detailed below.

However, we first wish to explore a potential mechanism for delayed HI production. Delayed loss of HI requires a mechanism capable of separating, in time, electron transfer from HI formation. We have demonstrated previously that electron capture at protonated arginine and lysine side chains is not equivalent.²¹ The hypervalent amine generated at lysine is not stable towards dissociative H-atom loss and therefore is not likely to be involved with delayed HI loss. In contrast, electron capture at protonated arginine creates a stable radical site by loss of a double bond. Theory was used to evaluate whether neutralized radical arginine side chain could attack the iodobenzyl functionality and initiate loss of HI. DFT calculations identified a reaction pathway proceeding by electron transfer from the neutral arginine side chain to the iodobenzene, followed by loss of iodide, and eventual formation of an ionic complex between I⁻ and protonated arginine side chain, see Scheme 2. The transition state for this pathway is only ~18 kJ/mol above reactants, and exhibits an elongated C-I bond and partially replanarized guanidinium. Upon completion, the reaction is exothermic and yields products ~-77 kJ/mol downhill from reactants. The system was calculated with freely translatable/rotatable functional groups and likely represents the lowest energy pathway (with respect to sterics). In an actual peptide, steric constraints would likely introduce additional barriers associated with rearrangement of the peptide structure to accommodate the transition state geometry. This pathway provides a viable mechanism for delayed HI production because transfer of the electron to the arginine side chain can be decoupled from subsequent attack of the iodobenzyl group by arginine. Importantly, the lysine analog, 4IB-YLKPPSFLK-NH₂, does not exhibit increased loss of HI following collisional activation (see SI Figure S2).

Intrigued by the idea that radical arginine side chain could initiate delayed HI loss in ETD/ECD, we examined other well-known dissociation pathways. Calculations reveal that radical arginine side chain can also initiate c/z backbone fragmentation and disulfide bond cleavage via pathways analogous to the one shown in Scheme 2. Complete details including

energetics and structures are shown in Figures S3, S4 of the supporting information. Backbone cleavage to yield *c/z* ions is slightly endothermic, though still possible with supplemental collisional activation. Disulfide bond fragmentation is exothermic and exposed by a minimal ~30 kJ/mol transition state. This pathway may contribute to the favored cleavage of disulfide bonds observed previously in ETD/ECD.³¹ These reaction pathways may contribute to the products observed following supplemental activation of ETnoD products.

Applications

The activation of carbon-iodine bonds by ETD as described above can be used to generate radicals site-specifically, enabling structurally sensitive RDD experiments that have advantages for isomer identification as described in the introduction. In the past these experiments were only possible by photoactivation of C-I bonds, but now it is clear that ETD may be used as well. Although in photodissociation-based experiments the fragment of interest is the loss of iodine, the equivalent radical generated by ETD is obtained by loss of HI. The difference occurs because electron transfer to a multiply protonated peptide yields a hydrogen abundant, odd-electron species. Loss of radical iodine from this odd electron ion would therefore yield an even-electron product. However, loss of HI, which is even electron, maintains the radical on the peptide. To test the structural sensitivity of fragmentation initiated by ETD-generated radicals, we conducted a series of experiments on peptide isomers, including epimers.

In vivo peptide/protein synthesis occurs exclusively from L-amino acids, but aging³² or enzymatic manipulations^{33,34} can lead to inversion of chirality for some residues. Peptides with a single D-amino acid are epimers of the all L-amino acid isomer, have identical exact masses, and are very difficult to identify. RDD initiated by photoactivation has been demonstrated previously to be the most sensitive method for epimer identification via comparison of the fragmentation spectra acquired independently from both epimers.¹² Given that ETD activation of carbon-iodine bonds leads to generation of both -HI and -I losses, it is possible to interrogate both radical and even-electron products simultaneously. Figure 4a shows results from collisional activation of the -I/-HI products from the L-Asp isomer of 4IB-VQEDFVEIHGK. Both side-chain losses that are unique to RDD and proton-mediated backbone cleavages leading to *b/y* ions from CID are observed in Figure 4a. In Figure 4b, the typical CID spectrum for the same peptide is shown, revealing preferential formation of *b/y* ions, as expected. The pure RDD spectrum, obtained in a separate experiment by photodissociation of the C-I bond followed by collisional activation, is shown in Figure 4c. The RDD spectrum is dominated by typical side-chain losses, accompanied by a few backbone cleavages. It is clear that a combination of the results from Figures 4b and 4c would yield the spectrum in Figure 4a, confirming that both even and odd-electron peptides can be fragmented simultaneously in the ETD-activation experiment.

ETD was used for iodo-activation of other isomers of 4IB-VQEDFVEIHGK including: L-isoAsp, D-Asp, and D-isoAsp. Figure 5 shows the ratios of the -HI/-I losses that are observed for each isomer. Although the largest peak corresponds to -I loss in each case, there are noticeable differences in the intensity of the -HI losses. For example, L-Asp

generates significantly less -HI loss than the D-isoAsp isomer. These results suggest that differences in the gas phase structures of the two isomers influence the interaction between the initial electron transfer site and the iodobenzyl group. Differences in the ratio of these two products could in theory be used directly for isomer identification, although clearly this strategy would not work for the D-Asp and D-isoAsp isomers in Figure 5. Fortunately, differences in the -HI/-I ratio between isomers should translate downstream to the subsequent activation step because the relative abundances of the even/odd-electron peptides will be different, altering the abundance of any products uniquely derived from either precursor. Therefore, these differences will still be relevant in the subsequent activation step, and the additional possibility for differential fragmentation will be simultaneously explored.

ETD-CID spectra for L-Asp and D-isoAsp 4IB-VQEDFVEIHGK are shown in Figure 6, and the corresponding R_{isomer} values are listed in Table 1. Interestingly, the largest R-value is obtained by comparing the b_9 ion to the -58K-4IB lysine side chain loss. The b_9 ion clearly originates from the even electron peptide (see Figure 4b). The side chain loss occurs due to RDD. The L-Asp isomer generates a smaller amount of radical precursor, as illustrated in Figure 5a. This likely contributes to the lower abundance of lysine side-chain loss for the L-Asp isomer in Figure 6a. The b_9 ion is most sensitive to structural differences between the isomers, but its abundance in Figure 6a may be augmented by the higher intensity of nonradical precursor.

The R_{isomer} values obtained from a variety of different activation methods for a several peptides are listed in Table 1. The ETD-CID method is not only competitive, but actually yields the highest value for 2/4 of the examined peptides. The high structural sensitivity derives from the ability of ETD-CID to leverage structural discrimination from both even and odd electron processes simultaneously.

Conclusions

ETD can be used to activate carbon-iodine bonds in a laser-free experiment, enabling access to RDD-like spectra. Observation of neutral iodine loss strongly indicates excited electronic states not populated directly by the transferred electron can be generated in ETD. Delayed loss of HI suggests that arginine is capable of “storing” the electron temporarily, allowing a variety of ETD-like fragmentation pathways to be accessed following subsequent additional collisional activation. ETD-generated radicals are capable of identifying peptide epimers, at times with greater sensitivity than other methods. The generation of both even- and odd-electron products, which can both be examined simultaneously, is a unique advantage of the ETD-activation method. It is clear that ion-ion reactions and radicals have many yet undiscovered uses that will continue to augment the capabilities of mass spectrometry in years to come.

Supplementary Material

Refer to Web version on PubMed Central for supplementary material.

Acknowledgments

The authors thank the NIH for financial support (NIGMS grant R01GM107099).

References

1. McAllister RG, Metwally H, Sun Y, Konermann L. Release of Native-like Gaseous Proteins from Electrospray Droplets via the Charged Residue Mechanism: Insights from Molecular Dynamics Simulations. *J Am Chem Soc.* 2015; 137(39):12667–12676. [PubMed: 26325619]
2. Zenobi R, Knochenmuss R. Ion Formation in MALDI Mass Spectrometry. *Mass Spectrom Rev.* 1998; 17(5):337–366.
3. Ly T, Julian RR. Residue-Specific Radical-Directed Dissociation of Whole Proteins in the Gas Phase. *J Am Chem Soc.* 2008; 130(1):351–358. [PubMed: 18078340]
4. Song T, Hao Q, Law C-H, Siu C-K, Chu IK. Novel C-Beta-C-Gamma Bond Cleavages of Tryptophan-Containing Peptide Radical Cations. *J Am Soc Mass Spectrom.* 2012; 23(2):264–273. [PubMed: 22135037]
5. Lee M, Kang M, Moon B, HBin Oh. Gas-Phase Peptide Sequencing by TEMPO-Mediated Radical Generation. *Analyst.* 2009; 134(8):1706–1712. [PubMed: 20448941]
6. Hodyss R, Cox HA, Beauchamp JL. Bioconjugates for Tunable Peptide Fragmentation: Free Radical Initiated Peptide Sequencing (FRIPS). *J Am Chem Soc.* 2005; 127(36):12436–12437. [PubMed: 16144360]
7. Gilbert JD, Fisher CM, Bu J, Prentice BM, Redwine JG, McLuckey SA. Strategies for Generating Peptide Radical Cations via Ion/ion Reactions. *J Mass Spectrom.* 2015; 50(2):418–426. [PubMed: 25800024]
8. Zhang X, Julian RR. Photoinitiated Intramolecular Diradical Cross-Linking of Polyproline Peptides in the Gas Phase. *Phys Chem Chem Phys.* 2012; 14(47):16243. [PubMed: 23111659]
9. Ly T, Julian RR. Elucidating the Tertiary Structure of Protein Ions in Vacuo with Site Specific Photoinitiated Radical Reactions. *J Am Chem Soc.* 2010; 132(25):8602–8609. [PubMed: 20524634]
10. Sun QY, Nelson H, Ly T, Stoltz BM, Julian RR. Side Chain Chemistry Mediates Backbone Fragmentation in Hydrogen Deficient Peptide Radicals. *J Proteome Res.* 2009; 8(2):958–966. [PubMed: 19113886]
11. Pham HT, Julian RR. Radical Delivery and Fragmentation for Structural Analysis of Glycerophospholipids. *Int J Mass Spectrom.* 2014; 370:58–65.
12. Tao Y, Julian RR. Identification of Amino Acid Epimerization and Isomerization in Crystallin Proteins by Tandem LC-MS. *Anal Chem.* 2014; 86:9733–9741. [PubMed: 25188914]
13. Ly T, Julian RR. Tracking Radical Migration in Large Hydrogen Deficient Peptides with Covalent Labels: Facile Movement Does Not Equal Indiscriminate Fragmentation. *J Am Soc Mass Spectrom.* 2009; 20(6):1148–1158. [PubMed: 19286394]
14. Cheng PY, Zhong D, Zewail AH. Kinetic-Energy, Femtosecond Resolved Reaction Dynamics - Modes of Dissociation (in Iodobenzene) from Time-Velocity Correlations. *Chem Phys Lett.* 1995; 237(5–6):399–405.
15. Agarwal A, Diedrich JK, Julian RR. Direct Elucidation of Disulfide Bond Partners Using Ultraviolet Photodissociation Mass Spectrometry. *Anal Chem.* 2011; 83(17):6455–6458. [PubMed: 21797266]
16. Ly T, Zhang X, Sun QY, Moore B, Tao YQ, Julian RR. Rapid, Quantitative, and Site Specific Synthesis of Biomolecular Radicals from a Simple Photocaged Precursor. *Chem Commun.* 2011; 47(10):2835–2837.
17. Zubarev RA, Kelleher NL, McLafferty FW. Electron Capture Dissociation of Multiply Charged Protein Cations. A Nonergodic Process. 1998; 7863(16):3265–3266.
18. Swaney DL, Wenger CD, Thomson JA, Coon JJ. Human Embryonic Stem Cell Phosphoproteome Revealed by Electron Transfer Dissociation Tandem Mass Spectrometry. *Proc Natl Acad Sci.* 2009; 106(4):995–1000. [PubMed: 19144917]

19. Chan WYK, Chan TWD, O'Connor PB. Electron Transfer Dissociation with Supplemental Activation to Differentiate Aspartic and Isoaspartic Residues in Doubly Charged Peptide Cations. *J Am Soc Mass Spectrom.* 2010; 21(6):1012–1015. [PubMed: 20304674]
20. Breuker K, Brüschweiler S, Tollinger M. Electrostatic Stabilization of a Native Protein Structure in the Gas Phase. *Angew Chem Int Ed.* 2011; 50(4):873–877.
21. Moore BN, Ly T, Julian RR. Radical Conversion and Migration in Electron Capture Dissociation. *J Am Chem Soc.* 2011; 133(18):6997–7006. [PubMed: 21495634]
22. Turek F, Julian RR. Peptide Radicals and Cation Radicals in the Gas Phase. *Chem Rev.* 2013; 113(8):6691–6733. [PubMed: 23651325]
23. Hood CA, Fuentes G, Patel H, Page K, Menakuru M, Park JH. *J Pept Sci.* 2008; 14:97–101. [PubMed: 17890639]
24. Tao WA, Zhang D, Nikolaev EN, Cooks RG. Copper(II)-assisted enantiomeric analysis of D,L-amino acids using the kinetic method: Chiral recognition and quantification in the gas phase. *J Am Chem Soc.* 2000; 122:10598–10609.
25. Frisch, MJ., Trucks, GW., Schlegel, HB., Scuseria, GE., Robb, MA., Cheeseman, JR., Scalmani, G., Barone, V., Mennucci, B., Petersson, GA., Nakatsuji, H., Caricato, M., Li, X., Hratchian, HP., Izmaylov, AF., Bloino, J., Zheng, G., Sonnenberg, JL., Hada, M., Ehara, M., Toyota, K., Fukuda, R., Hasegawa, J., Ishida, M., Nakajima, T., Honda, Y., Kitao, O., Nakai, H., Vreven, T., Montgomery, JA., Jr, Peralta, JE., Ogliaro, F., Bearpark, M., Heyd, JJ., Brothers, E., Kudin, KN., Staroverov, VN., Keith, T., Kobayashi, R., Normand, J., Raghavachari, K., Rendell, A., Burant, JC., Iyengar, SS., Tomasi, J., Cossi, M., Rega, N., Millam, JM., Klene, M., Knox, JE., Cross, JB., Bakken, V., Adamo, C., Jaramillo, J., Gomperts, R., Stratmann, RE., Yazyev, O., Austin, AJ., Cammi, R., Pomelli, C., Ochterski, JW., Martin, RL., Morokuma, K., Zakrzewski, VG., Voth, GA., Salvador, P., Dannenberg, JJ., Dapprich, S., Daniels, AD., Farkas, O., Foresman, JB., Ortiz, JV., Cioslowski, J., Fox, DJ. *Gaussian 09, Revision B.01.* Gaussian, Inc; Wallingford CT: 2010.
26. Hay PJ, Wadt WR. Ab Initio Effective Core Potentials for Molecular Calculations. Potentials for K to Au Including the Outermost Core Orbitals. *J Chem Phys.* 1985; 82(1):299.
27. Liu J, McLuckey SA. Electron Transfer Dissociation: Effects of Cation Charge State on Product Partitioning in Ion/ion Electron Transfer to Multiply Protonated Polypeptides. *Int J Mass Spectrom.* 2012; 330–332:174–181.
28. Shimamori H, Sunagawa T, Ogawa Y, Tatsumi Y. Low-energy electron attachment to C₆H₅X (X = Cl, Br and I). *Chem Phys Lett.* 1995; 232:115–120.
29. Hendricks NG, Lareau NM, Stow SM, McLean JA, Julian RR. Bond-Specific Dissociation Following Excitation Energy Transfer for Distance Constraint Determination in the Gas Phase. *J Am Chem Soc.* 2014; 136(38):13363–13370. [PubMed: 25174489]
30. Stephenson JL, McLuckey SA. Gaseous Protein Cations Are Amphoteric. *J Am Chem Soc.* 1997; 119(7):1688–1696.
31. Bishop A, Brodbelt JS. Selective Cleavage upon ETD of Peptides Containing Disulfide or Nitrogen–nitrogen Bonds. *Int J Mass Spectrom.* 2015; 378:127–133.
32. Truscott RJW, Schey KL, Friedrich MG. Old Proteins in Man: A Field in Its Infancy. *Trends Biochem Sci.* 2016; 41(8):654–664. [PubMed: 27426990]
33. Jia C, Lietz CB, Yu Q, Li L. Site-Specific Characterization of D-Amino Acid Containing Peptide Epimers by Ion Mobility Spectrometry. *Anal Chem.* 2014; 86(6):2972–2981. [PubMed: 24328107]
34. Bai L, Romanova EV, Sweedler JV. Distinguishing Endogenous D-Amino Acid-Containing Neuropeptides in Individual Neurons Using Tandem Mass Spectrometry. *Anal Chem.* 2011; 83(7):2794–2800. [PubMed: 21388150]

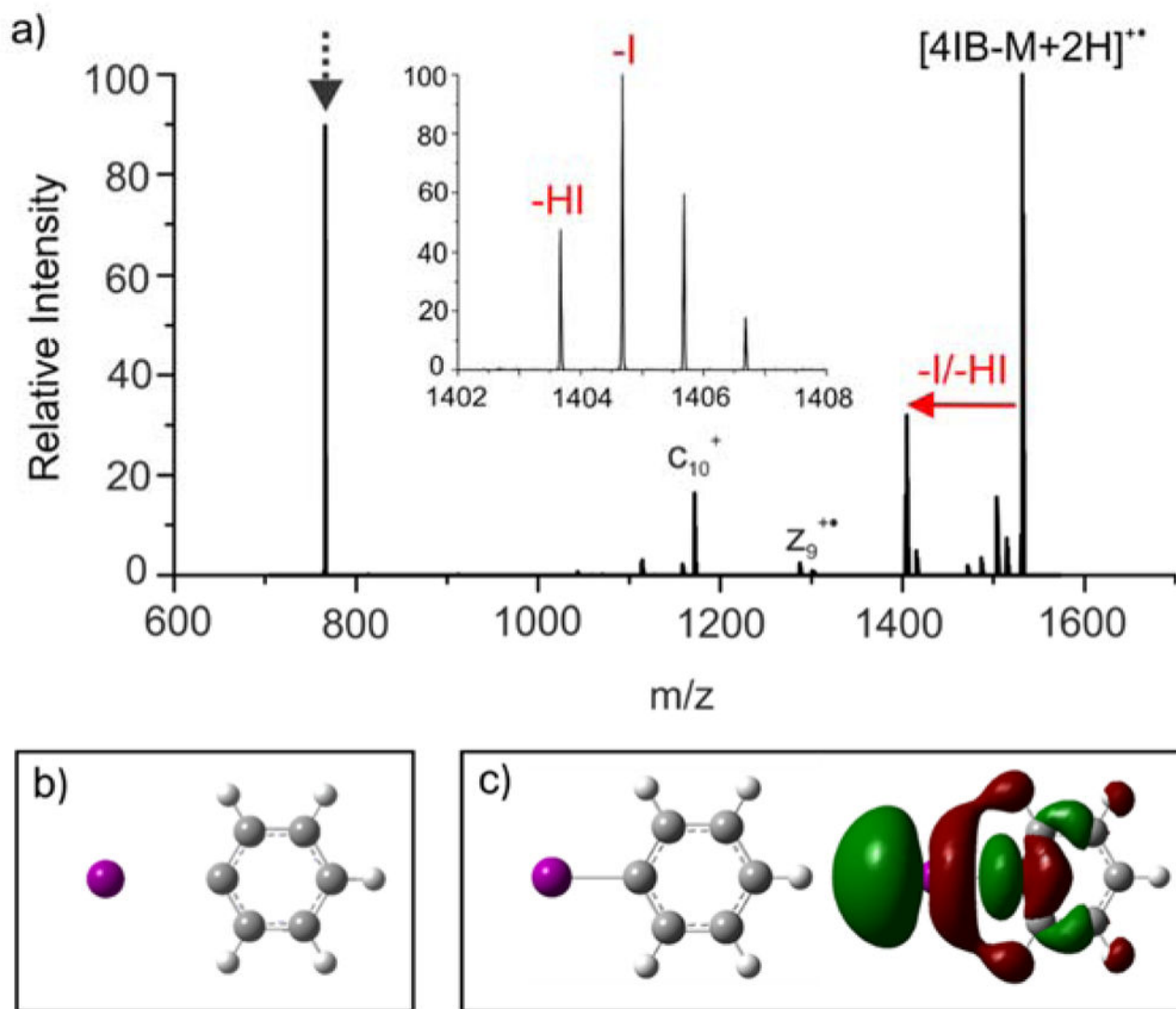


Figure 1.

a) ETD on $[4IB-VQEDFVEIHGK+2H]^{2+}$ leads to loss of $-HI/-I$. Inset shows the ratio of these losses. b) Addition of an electron to iodobenzene leads to spontaneous loss of iodide anion. c) Lowest unoccupied molecular orbital for iodobenzene is dissociative along the C-I bond.

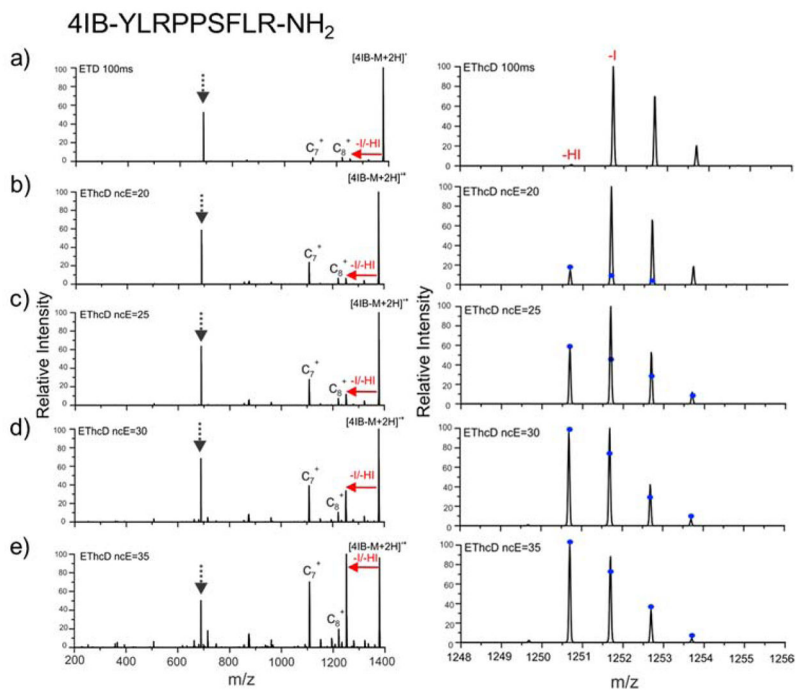


Figure 2. ETD on $[4\text{IB-YLRPPSF}_2\text{FLR-NH}_2+2\text{H}]^{2+}$ with increasing supplemental activation. $-I/-\text{HI}$ losses from the charge-reduced species are indicated by red arrows. The $-I/-\text{HI}$ losses are shown more clearly in zoomed in spectra on right. Blue dots represent the theoretical isotopic distribution for the $-\text{HI}$ peak that grows in, illustrating that the $-I$ peak does not increase with increasing supplemental activation.

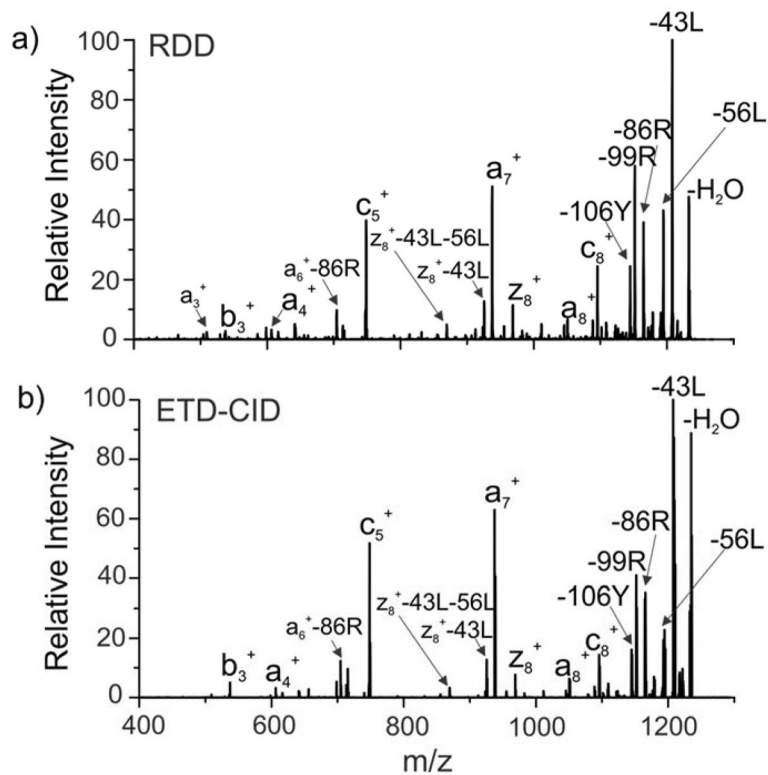


Figure 3. Comparison of the fragmentation spectra resulting from a) RDD on [4IB-YLRPPSFLR-NH₂+H]⁺ and b) ETD-CID on [4IB-YLRPPSFLR-NH₂-2H]²⁺. The spectra are very similar.

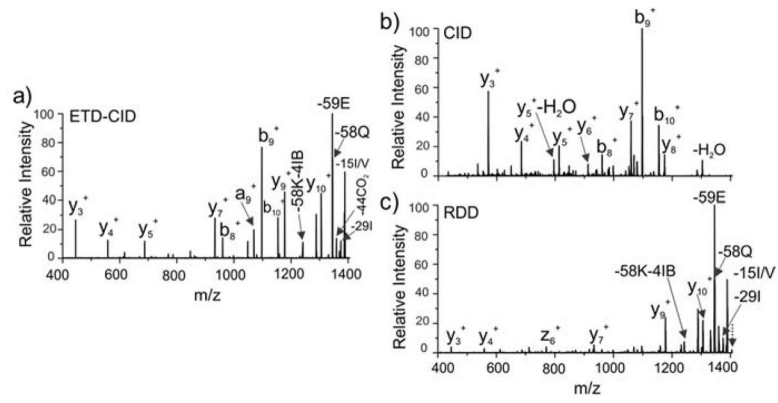


Figure 4.

- a). Collisional activation of –I/Hi products from ETD for protonated 4IB-VQEDFVEIHGK.
 b) CID spectrum. c) RDD spectrum.

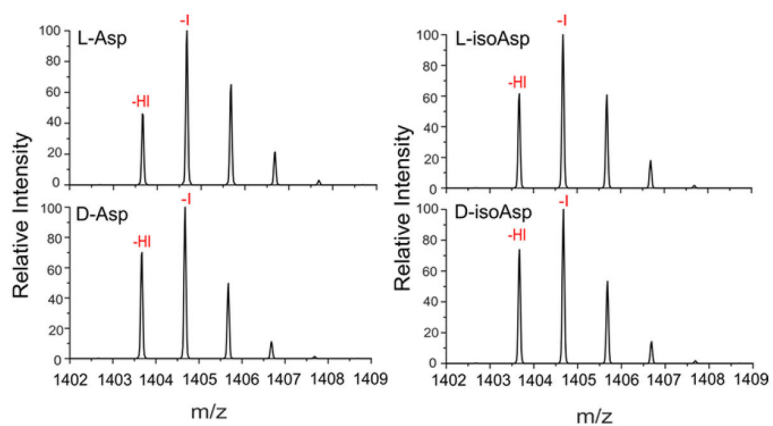


Figure 5. $-I/HI$ losses for listed isomers of protonated 4IB-VQEDFVEIHGK. The ratio of products is sensitive to isomer structure.

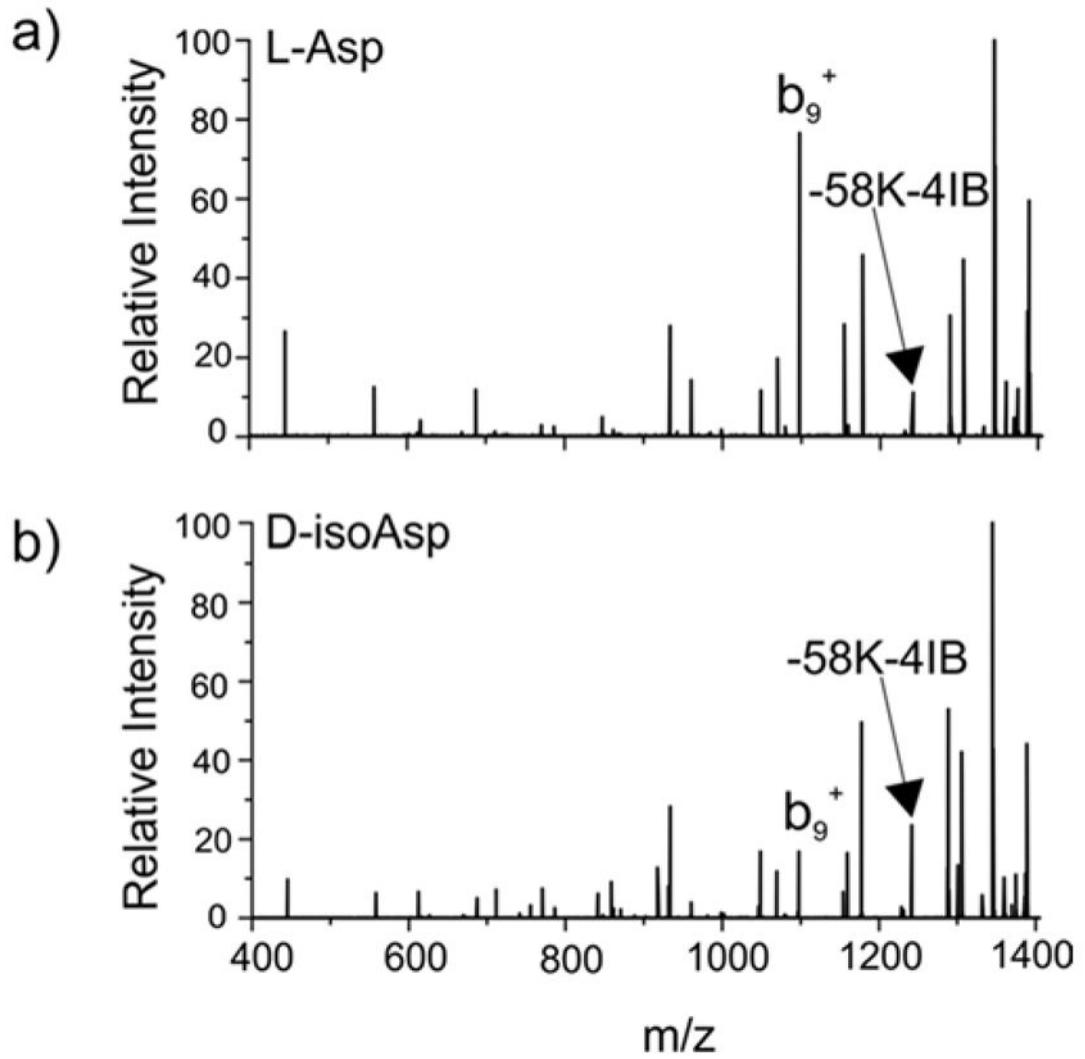
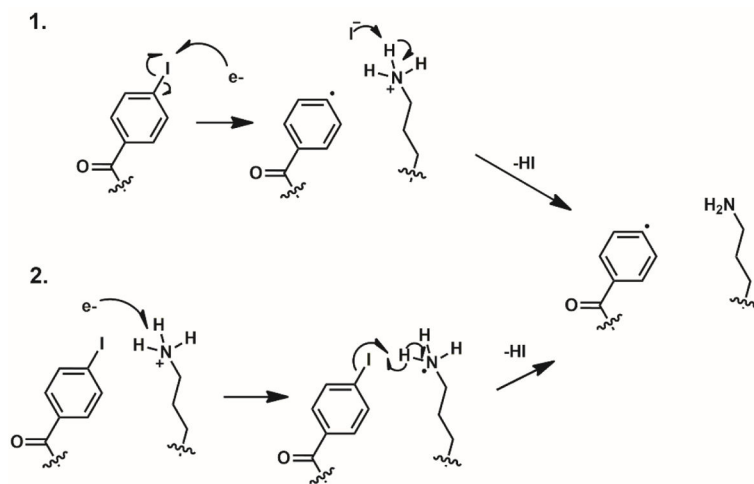
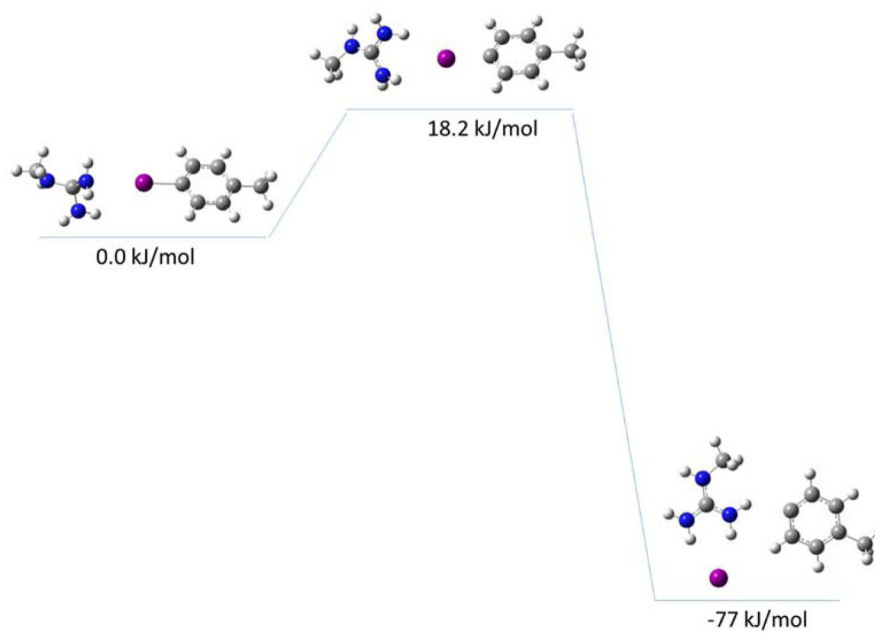


Figure 6. ETD-CID spectra for L-Asp and D-isoAsp isomers of protonated 4IB-VQEDFVEIHGK.



Scheme 1.
Two potential pathways that could account for observed loss of -HI.

**Scheme 2.**

Structures and transition states revealed by DFT calculations as described in the text.

Table 1

Peptide	R_{isomer}		
	CID	ETD-CID	RDD
^a VQEDFVEIHGK	8.1	7.0	3.5
^b VQEDFVEIHGK	2.7	6.7	8.7
^c VQEDFVEIHGK	4.6	9.6	3.6
Q DEHGFISR	2.0	3.0	1.8
HFSPE D LTVK	2.8	8.7	6.4
IQTGL D ATHAER	1.3	2.0	3.0

^a) Aspartic acid in red represents L-Asp vs D-Asp

^b) Italicized aspartic acid represents L-Asp vs L-isoAsp

^c) Bold aspartic acid represents L-Asp vs D-isoAsp